Submitted: 11 May, 2023 Accepted: 10 August, 2023 Online Published: 17 April, 2024 DOI:10.22514/ejgo.2024.040

ORIGINAL RESEARCH

European Journal of Gynaecological Oncology

Metabolism related gene signature predicts prognosis and indicates tumor immune infiltration in ovarian cancer

Yaodong Zhang[1,†], Xuenan Zhao[2,†], Huilan Qiu[1,†], Xia Chen[3], Zhongwei Zhang[1], Biao Zhu[1], Liwen Bu[4,5,*], Zuguang Xia[6,*]

[1]Department of Critical Care, Fudan University Shanghai Cancer Center, 200032 Shanghai, China
[2]Department of Urology, Fudan University Shanghai Cancer Center, 200032 Shanghai, China
[3]Department of Neurology, Renji Hospital, Shanghai Jiao Tong University School of Medicine, 200001 Shanghai, China
[4]Department of Nursing Administration, Fudan University Shanghai Cancer Center, 200032 Shanghai, China
[5]Department of Colorectal Surgery, Fudan University Shanghai Cancer Center, 200032 Shanghai, China
[6]Department of Medical Oncology, Fudan University Shanghai Cancer Center, 200032 Shanghai, China

***Correspondence**
xiazg@shca.org.cn
(Zuguang Xia);
boliwen68@shca.org.cn
(Liwen Bu)

† These authors contributed equally.

Abstract

Energy metabolism plays a crucial role in supporting cancer cell growth and driving tumor progression. Our objective was to create a unique gene signature based on metabolic genes that could accurately predict the prognosis of patients with ovarian cancer (OC). We accessed microarray data of patients with OC from The Cancer Genome Atlas (TCGA) and Gene Expression Omnibus (GEO) databases. Patients from the TCGA dataset were divided into training and internal validation sets, maintaining a ratio of 3:1. Based on Least absolute shrinkage and selection operator Cox regression analysis, twenty-nine metabolism-related genes were identified for the development of the metabolic signature. Patients in the training set were successfully divided into low- and high-risk groups with a significantly different prognosis (Hazard Ratio (HR): 2.76, 95% Confidence Interval (CI): 2.12–3.59, $p < 0.001$). The prognostic value of this signature was confirmed in the internal (HR: 3.06, 95% CI: 1.80–5.17, $p < 0.001$) and external validation sets (HR: 2.17, 95% CI: 1.57–2.99, $p < 0.001$). The time-dependent receiver operating characteristic (ROC) at the 5-year interval demonstrated that the prognostic accuracy of this metabolic signature (Area under curve (AUC) = 0.723) was superior to that of any other clinicopathological features, including the Federation of Gynecology and Obstetrics stage (AUC = 0.509), grade (AUC = 0.536), and debulking status (AUC = 0.637). Further immune cell infiltration analysis showed that low-risk patients had a higher enrichment of immune-activating cells. In conclusion, a novel metabolic signature with good performance was established in this study. This prognostic model could aid in the identification of high-risk patients who require aggressive follow-up and therapeutic strategies.

Keywords

Ovarian cancer; TCGA; GEO; Metabolism; Prognosis

1. Introduction

Ovarian cancer (OC) is one of the most common and lethal cancers of the female reproductive system worldwide [1]. Despite advances in treatment strategies over the past few decades, cure rates remain relatively unchanged and the overall survival (OS) of patients remains low. Currently, the American Joint Committee on Cancer Tumor-Nodal-Metastasis (TNM) and FIGO staging system is still the dominant risk evaluation method used [2]. However, the prognostic accuracy of this system is poor, and the prognosis of patients at the same stage varies significantly. Therefore, it is essential to identify highly specific and sensitive prognostic biomarkers for the detection of high-risk patients who require more aggressive therapeutic interventions.

Increasing evidence suggests that multigene-based gene signatures are promising prognosis prediction models for OC [3–10]. However, despite having had several multigene signatures established for OC, their prognostic accuracy remains weak. Therefore, a robust gene signature with considerable predictive performance is required.

Cancer cells share the common phenotype of uncontrolled cell proliferation and must efficiently generate the energy and macromolecules required for cellular growth [11]. Previous studies confirmed that metabolic reprogramming during tumor initiation and progression is critical for all cancer cells. Accumulating evidence revealed that aerobic glycolysis, metabolic symbiosis, glutamine metabolism, enhanced lipogenesis, and redox stress are important metabolic reprogramming features crucial for cancer progression [12–16]. In addition, many critical enzymes or transporters that mediate these processes are prognostic biomarkers of OC [17–24]. For instance, hexokinase 2 and glyceraldehyde-3-phosphate dehydrogenase regulate mTOR and apoptosis in OC [25]. Additionally, as a critical regulator of hypoxia-induced glycolysis, Glucose transporter-1 (GLUT1) is associated with angiogenesis and epidermal

growth factor signaling in OC [26]. However, no previous studies have comprehensively analyzed these metabolism-related genes in OC. A multigene signature based on metabolic genes may have superior prognostic accuracy in predicting cancer prognoses.

In the present study, 855 patients with OC who had complete follow-up information and microarray data were identified from The Cancer Genome Atlas (TCGA) and Gene Expression Omnibus (GEO) databases. Based on the univariate and least absolute shrinkage and selection operator (LASSO) Cox regression models, a robust metabolic signature with considerable prognostic accuracy was established for OC.

2. Methods

2.1 Datasets

Microarray information generated *via* the Affymetrix Human Genome U133A Array platform was acquired from the TCGA database (https://genome-cancer.ucsc.edu). Patients exhibiting both transcriptome data and comprehensive follow-up records were identified. Subsequently, three additional microarray datasets (GSE14764, GSE26712 and GSE23554), generated using the same platform, were procured from the GEO database and amalgamated to form an external validation cohort. Corresponding Entrez Gene identifiers were employed to map all probes [27]. In cases where multiple probes were associated with a specific Entrez Gene identifier, the mean value was computed to ascertain the average expression level. To address potential batch variations across distinct microarray datasets, the ComBat method was employed.

2.2 Metabolism-related gene set

A total of 5557 human energy metabolism-related genes were downloaded from The Human Metabolome Database (http://hmdb.ca/).

2.3 Identification of prognostic metabolic genes

To form our training dataset, we randomly allocated patients sourced from the TCGA database into either the training or validation groups, adhering to a 3:1 ratio. Within the training set, we carried out an initial univariate Cox survival analysis. This analysis enabled us to evaluate the prognostic relevance of metabolic genes and pinpoint those that exhibit prognostic associations. The LASSO Cox regression model at a ten-fold cross-validation was used to identify the most important prognosis-related metabolic genes [28].

2.4 Construction of the metabolic risk score

Employing LASSO Cox regression analysis, we ascertained a definitive roster of metabolic genes that hold significance in constructing a multi-gene signature. Employing a standardized formula for risk score calculation, we computed individual risk scores by amalgamating the gene expression values with their respective LASSO Cox regression coefficients for each patient. With reference to the median risk score established within the training cohort, patients were stratified into groups characterized by low and high risk.

2.5 Functional annotation

To identify differentially expressed genes (DEGs) between the low- and high-risk patients, the Linear Models for Microarray data (LIMMA) method was used. The threshold for significance was set at an adjusted p value < 0.05 and fold change >1.5. Furthermore, functional annotation of Kyoto Encyclopedia of Genes and Genomes (KEGG)/Gene ontology (GO) biological process enrichment was performed using the clusterProfiler R package.

2.6 Immune infiltration analysis

We employed the Cell-type Identification by Estimating Relative Subsets of RNA Transcripts (CIBERSORT) deconvolution approach to evaluate the relative abundance of 22 tumor-infiltrating immune cells in each sample. These included naïve and memory B cells, plasma cells, Cluster of Differentiation (CD)8 and CD4 T cells, naïve T cells, CD4 memory resting and activated T cells, follicular helper T cells, regulatory T cells, $\gamma\delta$ T cells, resting and activated natural killer (NK) cells, monocytes, M0–M2 macrophages, resting and activated dendritic cells, resting and activated mast cells, eosinophils and neutrophils.

2.7 Statistical analysis

For contrasting survival disparities among the two survival curves, we employed Kaplan-Meier survival plots in conjunction with log-rank tests. To assess prognostic precision, we carried out time-dependent receiver operating characteristic (ROC) analysis, with the area under the curve (AUC) serving as an indicator of predictive efficacy. In cases where the data exhibited skewed distribution, the Wilcoxon rank-sum test was utilized; meanwhile, for normally distributed data, differences between groups were assessed using Student's t-test. We used R software (version 3.2.5; www.r-project.org) for all statistical analyses.

3. Results

3.1 Development and definition of the metabolic signature

A total of 422 patients with OC from the TCGA dataset were divided into a training set, and the remaining 140 patients included in the internal validation set. Basic clinicopathological information of the patients from the TCGA and GEO datasets is shown in Table 1. Initially, we performed univariate Cox survival analysis and identified 97 metabolic genes ($p < 0.01$; **Supplementary Table 1**). Then, the LASSO Cox regression model was used to screen these metabolic genes, whereafter 29 were identified as part of the metabolic signature for OC (Fig. 1). Finally, the risk score was calculated based on the expression values of the 29 genes and risk regression coefficients for each patient. The risk regression coefficients for the 29 genes are listed in **Supplementary Table 2**.

TABLE 1. Basic information of patients from TCGA and GEO datasets.

	Discovery set (N = 422)	Internal validation (N = 140)	External validation (N = 293)
FIGO stage			
I	8	7	8
II	21	6	1
III	332	100	69
IV	59	25	2
Debulking status			
Optimal	83	32	154
Suboptimal	297	89	135
Grade			
Low grade	57	18	52
Moderate/High grade	357	117	239

FIGO: Federation of Gynecology and Obstetrics.

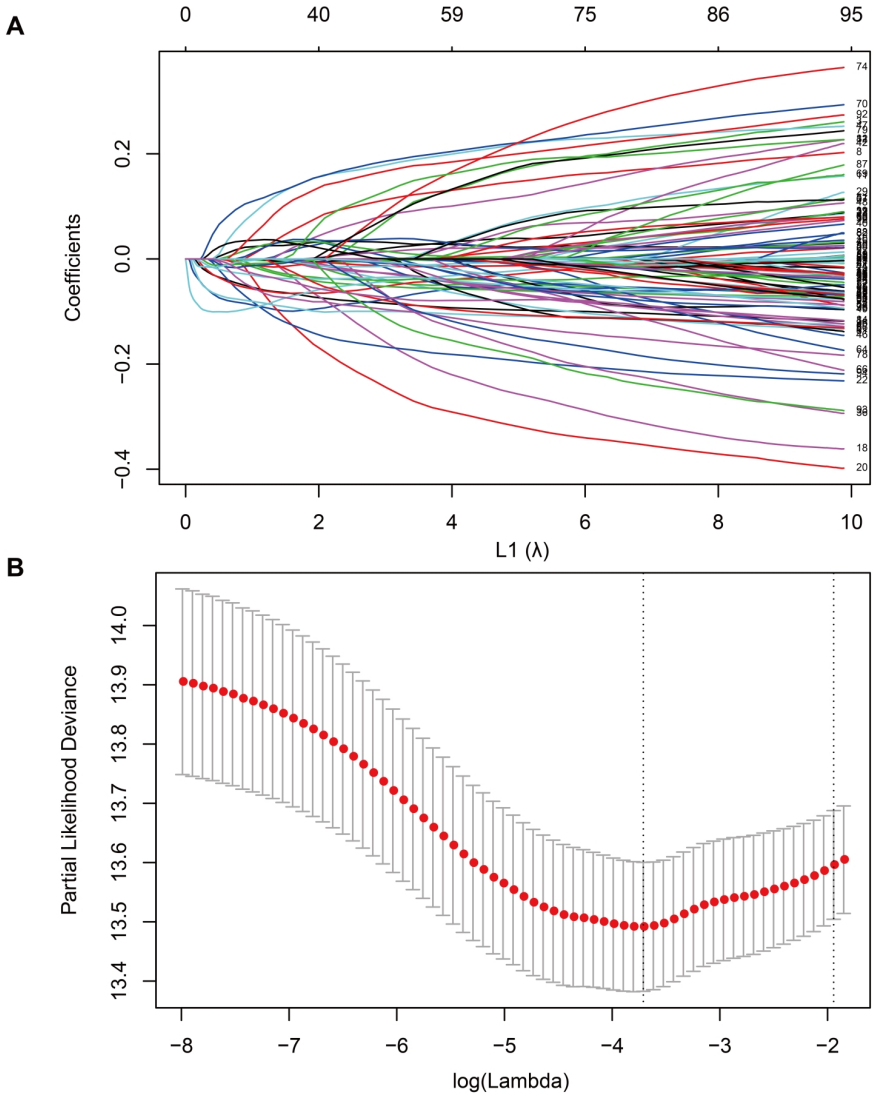

FIGURE 1. Selection of prognostic metabolic genes based on Least Absolute Shrinkage and Selection Operator (LASSO) Cox model. (A) Profiles of the coefficients obtained through the LASSO for the 98 metabolic genes associated with overall survival (OS). (B) Selection of the tuning parameter (λ) in the LASSO model utilizing tenfold cross-validation with the minimum criterion.

3.2 Performance of the metabolic signature in the training set

According to the median risk score, the patients were stratified into two distinct risk groups: low- and high-risk groups. Notably, as depicted in Fig. 2A (left panel), the distribution of risk scores exhibited a compelling association with the occurrence of adverse events leading to death, indicating that patients with higher risk scores had a distinctly elevated likelihood of experiencing mortality. To comprehensively evaluate the prognostic accuracy of the identified metabolic signature, time-dependent ROC analysis was performed, which robustly demonstrated its exceptional discriminative power in predicting OS at multiple critical temporal landmarks, including at 1-, 3- and 5-year intervals (Fig. 2A, middle panel). Furthermore, leveraging the versatility of the Kaplan-Meier survival plot with the log-rank test, we confirmed that patients classified in the high-risk category exhibited significantly inferior OS outcomes compared with their counterparts in the low-risk group (Fig. 2A, right panel). Furthermore, survival rates of patients within the low-risk stratum were documented to be 93.5%, 81.2% and 53.8% at the 1-, 3- and 5-year intervals, respectively. In striking contrast, patients allocated to the high-risk group demonstrated notably poorer survival rates, recorded at 90.4%, 52.1% and 18.1% for the respective time intervals (HR: 2.76, 95% CI: 2.12–3.59, $p < 0.001$; Fig. 2A, right panel).

3.3 Validation of the metabolic signature

The previous results were validated using an external validation set. As expected, patients in the high-risk group presented significantly poorer OS rates compared with those cases in the low-risk group (HR: 3.06, 95% CI: 1.80–5.17, $p < 0.001$; Fig. 2B, right panel). The 1-, 3- and 5-year OS rates in the low-risk group were 97.8%, 69.1% and 58.8%, respectively, and those in the high-risk group were 85.8%, 49.0% and 17.4%, respectively.

The same analysis was performed on the external validation cohort. In total, 293 patients with OC from the GSE14764, GSE26712 and GSE23554 datasets were identified to validate the prognostic value of the developed metabolic signature. Based on the cutoff point determined in the training set, 138 (58.0%) patients were classified as low risk and 155 (31.6%) as high risk. Consistent with results of the training and internal validation sets, this signature performed well in predicting OS (Fig. 2C, middle panel) and could separate patients into low- and high-risk groups with significantly different OS rates (HR: 2.17, 95% CI: 1.57–2.99, $p < 0.001$; Fig. 2C).

3.4 Subgroup and prognostic accuracy analyses of the metabolic signature

To test the independence of the developed metabolic signature in predicting OS rates, multivariate Cox regression analysis was performed for the training, internal validation, and external validation sets. The results suggest that this metabolic signature was independently associated with OS in the training and validation sets (Table 2). Further stratified analysis showed that this metabolic signature was a robust prognostic factor in patients with different tumor stages, grades, and debulking statuses (Fig. 3).

To further compare the prognostic accuracy of the metabolic signature with that of other clinicopathological factors, survival ROC analysis was performed (Fig. 4). The results confirmed that the metabolic signature (AUC = 0.723) performed better than any other tested factor, including the FIGO stage (AUC = 0.509), grade (AUC = 0.536), and debulking status (AUC = 0.637).

3.5 Construction of the metabolic signature-based nomogram

Following meticulous adjustment for other pertinent clinicopathological variables, our analyses unequivocally substantiated that the metabolic signature, along with debulking status, retained their status as two robust, independent prognostic factors within the entire cohort under investigation (Fig. 5A). To enhance the clinical applicability and usability of this highly promising prognostic signature, we meticulously constructed a comprehensive nomogram based on insights gleaned from the multivariate analysis (Fig. 5B). Crucially, this meticulously devised nomogram seamlessly integrates the dynamically informative contributions of the metabolic signature and debulking status, which could holistically empower clinicians with a valuable tool for personalized prognostic assessments.

3.6 Pathway enrichment and immune characteristics of the metabolic signature

To identify DEGs between low- and high-risk patients, the LIMMA method was used, and a total of 77 genes with fold change >1.5 and FDR <0.5 identified (**Supplementary Table 3**). Then, GO/KEGG enrichment analysis was performed and showed that the metabolic signature was significantly associated with the tumor metastasis-related biological process or various pathways, including extracellular matrix organization, extracellular structure organization, extracellular matrix-receptor interaction, and the Transforming Growth Factor-beta signaling pathway (Fig. 6A–D). Furthermore, we performed CIBERSORT analyses to characterize immune cell infiltration in patients (Fig. 7A). By comparing the infiltrating cells between low- and high-risk patients, we observed that activated dendritic cells, M1 macrophages, T follicular helper cells, and $\gamma\delta$ T cells were notably enriched in the low-risk patients (Fig. 7B).

4. Discussion

Despite advancements in treatment strategies over the past decades, the 5-year OS rate of patients diagnosed with OC remains less than 50%. Death risk evaluation of patients prior to treatment may enable risk-adjusted therapeutic intervention and hence offer an improved, individualized treatment and follow-up scheme. Generally, high-risk patients can be channeled into trials involving aggressive therapies. However, no robust risk stratification tools have been established to predict the prognosis of OC. In the present study, a novel and robust prognostic signature incorporating 29 metabolism-related genes was established to improve death risk assessment for patients with OC. The prognostic value of this metabolic

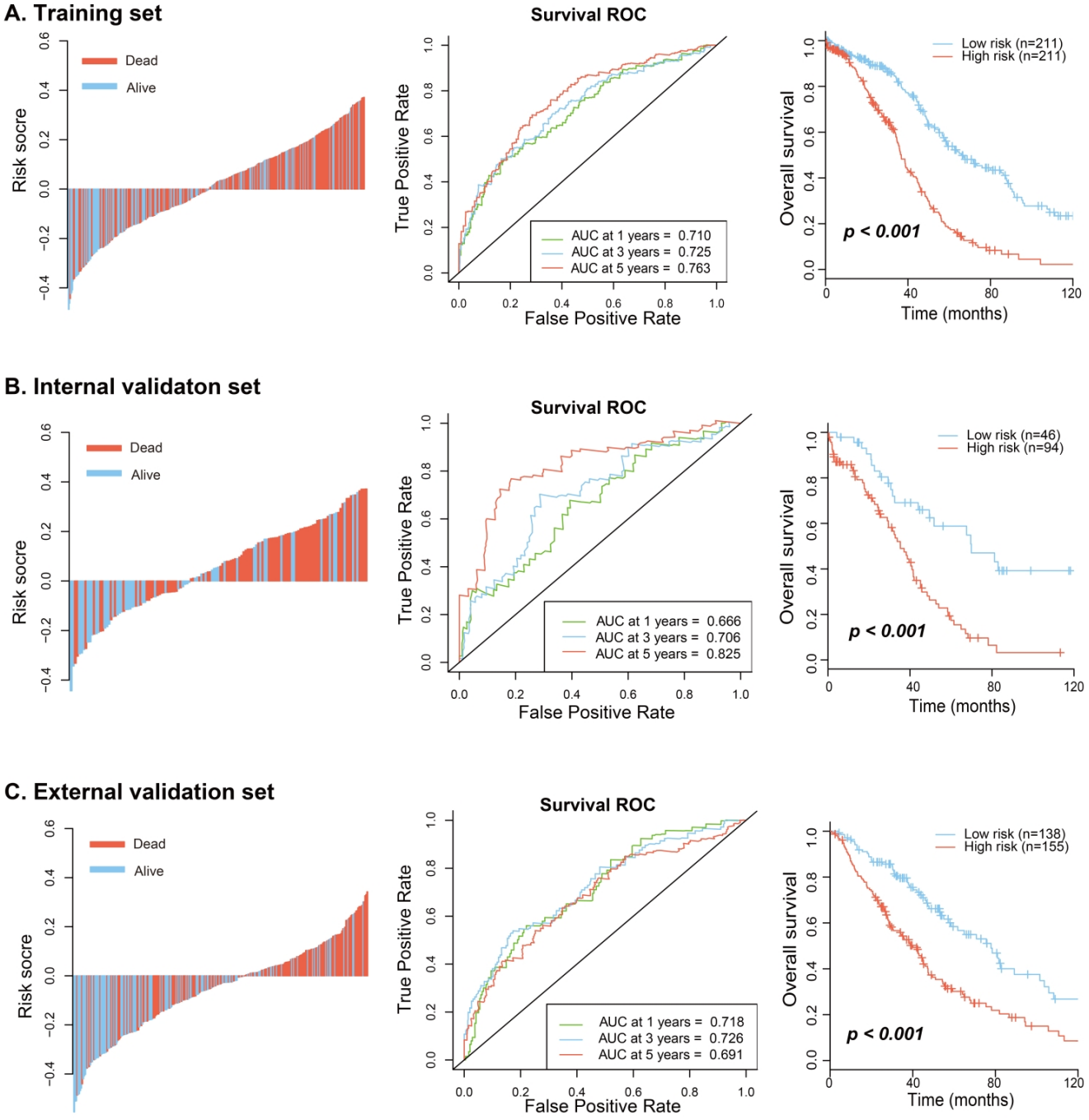

FIGURE 2. Performance of metabolic signature in training, internal validation and external validation. (A) Distribution of risk scores for mortality, survival receiver operating characteristic (ROC) curves at intervals of 1, 3 and 5 years, and Kaplan-Meier survival plots for patients categorized into low- and high-risk groups within the training dataset. (B) Equivalent analyses conducted in the internal validation dataset. (C) Corresponding assessments performed within the external cohort. AUC: area under the curve.

TABLE 2. Multivariate Cox regression analysis of metabolic signature in predicting OS.

	HR	*p**
Training set	22.99 (10.56–50.09)	<0.001
Internal validation set	7.87 (1.78–34.68)	0.006
External validation set	27.55 (9.84–77.09)	<0.001

**Adjusting for FIGO stage, grade and debulking status. HR: Hazard Ration; FIGO: Federation of Gynecology and Obstetrics.*

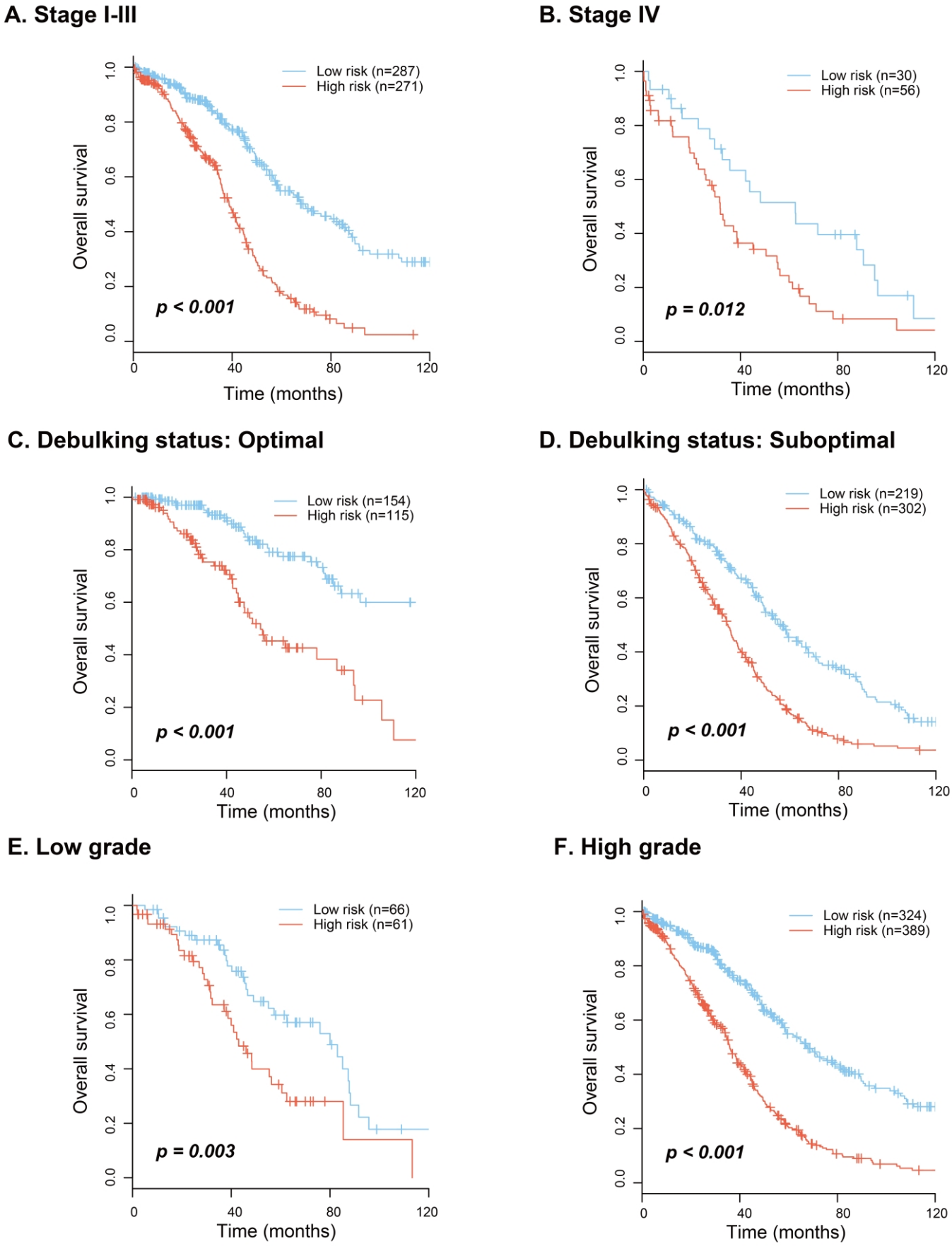

FIGURE 3. Kaplan-Meier survival analysis of the metabolic signature in the entire dataset (N = 855) stratified by the FIGO stage (A,B), debulking status (C,D), and histological grade (E,F).

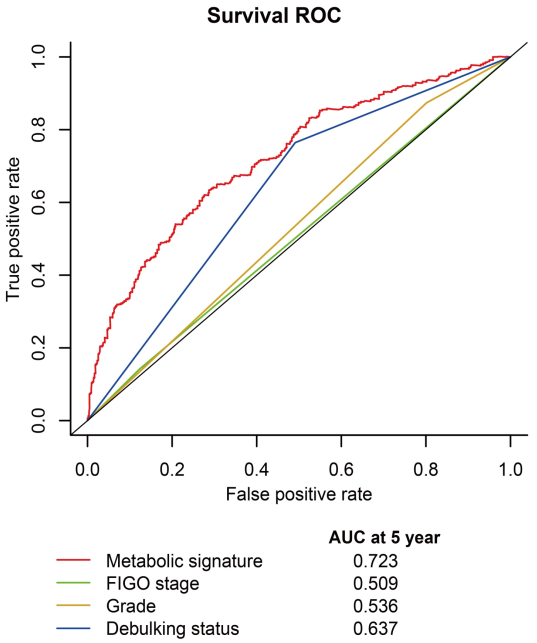

FIGURE 4. Time-dependent receiver operating characteristic (ROC) curves evaluated at the 5-year interval, showcasing the performance of the metabolic signature, debulking status, FIGO stage, and tumor grade within the complete cohort. AUC: area under the curve; FIGO: Federation of Gynecology and Obstetrics.

A

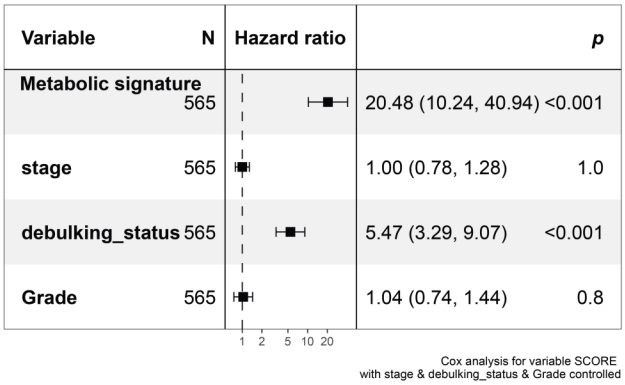

B

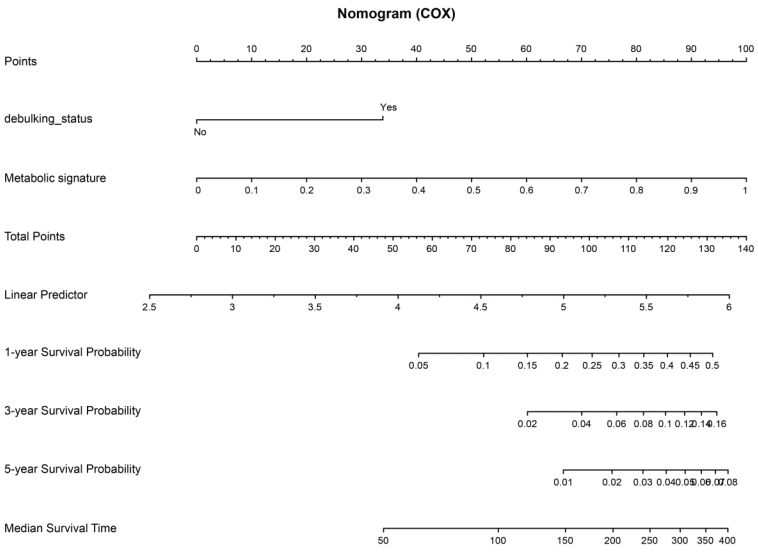

FIGURE 5. Multivariate Cox regression and analysis and clinical nomogram. (A) Multivariate Cox regression analysis results in patients with ovarian cancer (OC). (B) Prognostic nomogram integrating the metabolic signature and debulking status.

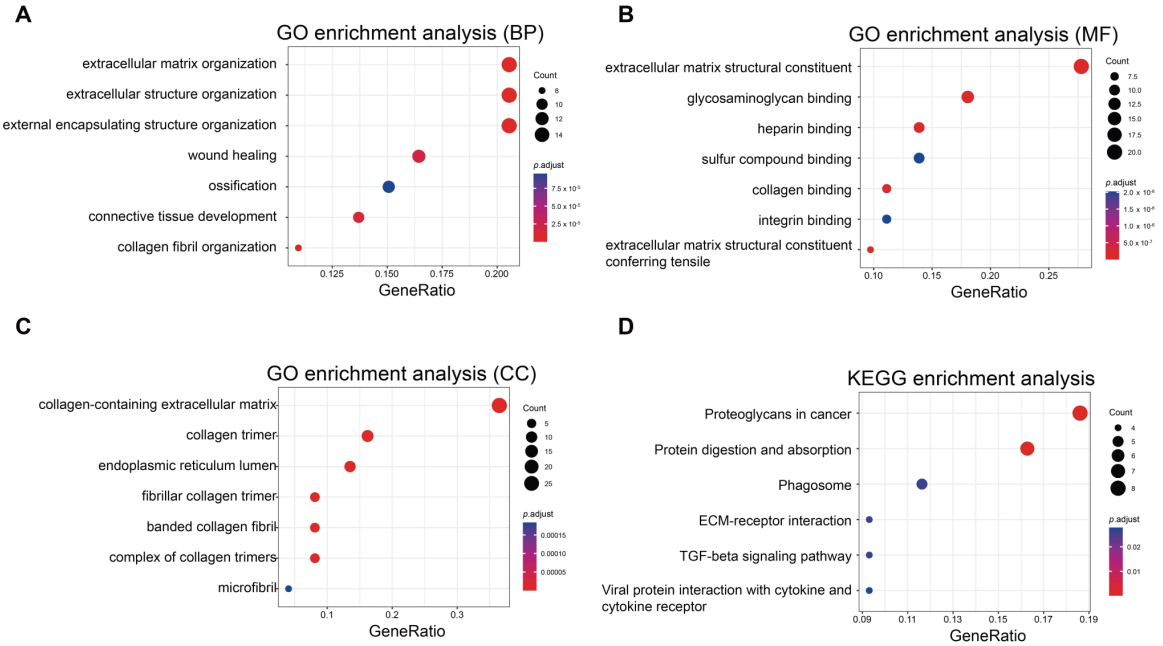

FIGURE 6. Functional annotation of GO/biological process (A), GO/molecular function (B), GO/cellular component (C), and KEGG (D) based on differentially expressed genes (DEGs) between the low- and high-risk patients. GO: Gene ontology; BP: Biological process; MF: Molecular function; CC: Cellular Component; KEGG: Kyoto Encyclopedia of Genes and Genomes; ECM: extracellular matrix; TGF: Transforming Growth Factor.

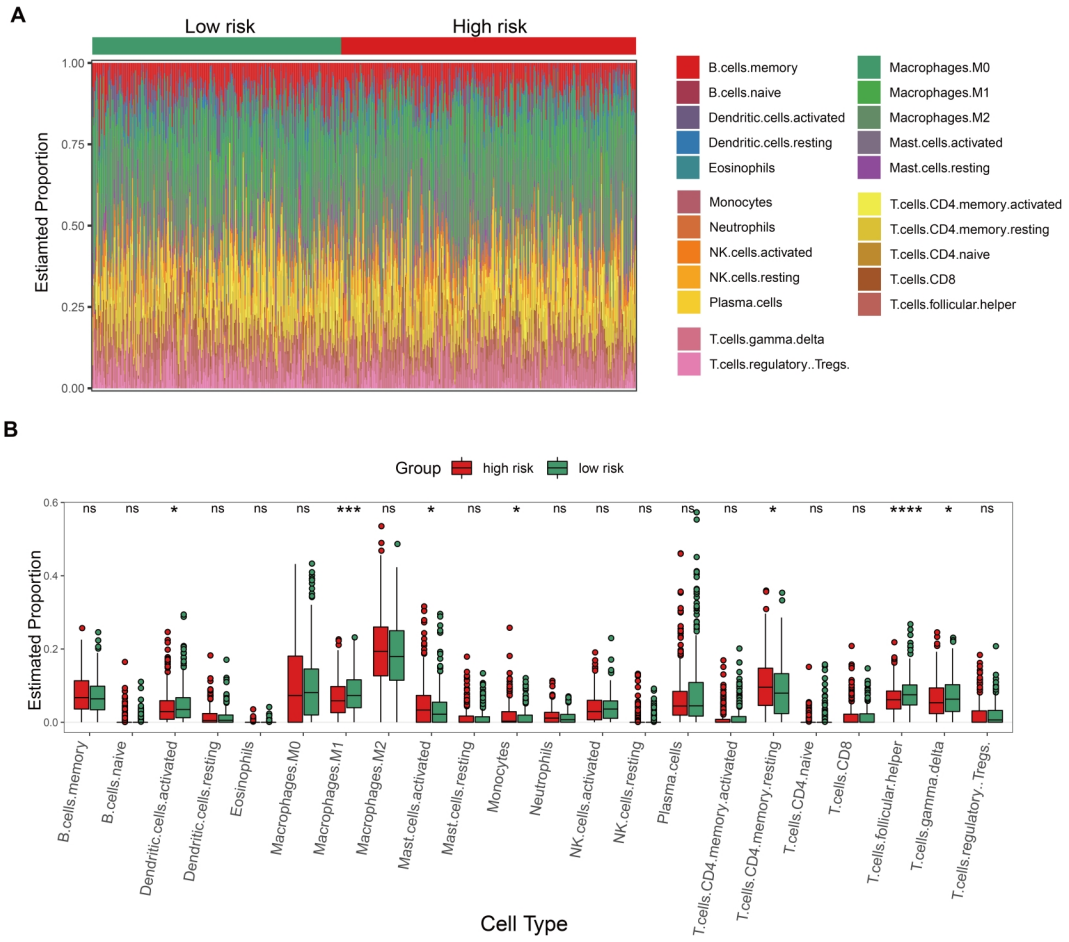

FIGURE 7. Immune cell infiltration analysis between low and high risk groups. (A) Analysis depicting the immune cell infiltration profile within ovarian cancer (OC) tissues. (B) Boxplot illustrating the immune cell proportions determined *via* CIBERSORT analysis. NK: Natural killer; CD: Cluster of Differentiation.

signature determined in the training set was successfully validated in the internal and external validation sets, suggesting good reproducibility in predicting OS for patients with OC. Further, multivariate and subgroup analyses based on FIGO stage, debulking status, and histological grade showed that this biomarker was an independent prognostic factor for OS in OC. Additionally, prognostic accuracy analysis based on time-dependent ROC curves revealed the best results for the metabolic signature among the other clinicopathological features, suggesting that incorporating it into the current risk evaluation system could notably improve the prediction of long-term survival. Based on the TCGA data, Chen *et al*. [5] proposed a new consensus ovarian subtype classifier for high-grade serous ovarian carcinoma. Although this subtyping classifier exhibited moderate pairwise concordance across our data compendium and was associated with OS in a meta-analysis across datasets, its performance in predicting OS in patients with OC is inferior to the metabolic signature developed in this study.

Most of the metabolism-related genes incorporated into this signature have been previously studied in OC and validated as prognostic factors. Phosphoglycerate dehydrogenase (*PHGDH*) mediates the biosynthesis of serine from glucose, which is one of the most studied metabolic pathways and has been shown to be linked to platinum resistance in OC [29]. *ALDH5A1* is an A1 member of the aldehyde dehydrogenase 5 superfamily, and its expression was downregulated in patients with OC. It was found that a high level of *ALDH5A1* is associated with improved OS rates [30]. Annexin A4 (*ANXA4*) is highly expressed in OC, and its knockdown can result in significant growth retardation and greater sensitivity to carboplatin in OC cells [31]. Asparaginase-like 1 (*ASRGL1*) is overexpressed in OC and closely associated with cell growth and apoptosis [32]. The receptor tyrosine kinase, AXL, was found to be primarily expressed in advanced-stage OC, and inhibition of its signaling results in decreased invasion and matrix metalloproteinase activity, thus inhibiting tumor metastasis potential [33]. Frizzled Class Receptor 10 (*FDZ10*) mRNA stability is correlated with upregulation of the Wnt/β-catenin pathway and contributes to peroxisome proliferator activated receptor inhibitor resistance in OC [34]. The *N*-acetylgalactosaminyltransferase 6 (*GALNT6*) enzyme that mediates the initial step of mucin type-O glycosylation enhances aggressive phenotypes in OC cells by regulating epidermal growth factor receptor activity [35]. Glutathione S-transferase Zeta 1 (*GSTZ1*) has been previously reported as a prognostic gene in OC [36]. Microfibril-associated Protein 4 (*MFAP4*) is highly expressed in OC, and its high expression levels predict chemotherapy sensitivity and are significantly associated with poor prognosis in patients with OC [37]. Solute Carrier Family 7 Member 11 (*SLC7A11*), which mediates cystine-glutamate exchange, could serve as an indicator of the cellular response to chemotherapy, offering a potential target for increasing the chemotherapy response to multiple drugs [38]. Transglutaminase 2 (*TGM2*) was shown to play a crucial role in the regulation of doxorubicin/cisplatin resistance in OC [39]. Regarding the other metabolism-related genes included in our signature, further clinical and basic research should be performed to unveil their prognostic value and molecular functions in OC.

By comparing the infiltrating cells between low- and high-risk patients, we observed that activated dendritic cells, M1 macrophages, T follicular helper cells, and $\gamma\delta$ T cells were notably enriched in the low-risk patients. Immune cell infiltration plays a critical role in tumor development, progression, and response to therapy. Immune cells, such as cytotoxic T and natural killer cells, can recognize and eliminate cancer cells, functioning as a defense mechanism against tumor growth. This immune surveillance is crucial to prevent the expansion and spread of cancer cells. Based on these results, we propose that antitumor immunity may be highly activated in low-risk patients.

This was the first study to comprehensively analyze the prognostic value of metabolism-related genes in OC and to develop a novel metabolic signature for predicting OC risk. However, this study had several limitations. First, all data used were obtained from public databases, and prospective validation based on polymerase chain reaction data is needed. Second, several important parameters, such as detailed chemotherapy regimens and histological type, were not available in the public databases. Lastly, the mechanisms underlying the involvement of metabolic genes in OC progression requires further investigated.

5. Conclusions

In conclusion, a novel metabolic signature with good performance was established in this study. This prognostic model could aid in the identification of high-risk patients requiring aggressive follow-up and therapeutic strategies.

AVAILABILITY OF DATA AND MATERIALS

Source data and reagents are available from the corresponding author upon reasonable request.

AUTHOR CONTRIBUTIONS

LWB and ZGX—Conception and design. YDZ, XNZ and HLQ—Administrative support; Provision of study materials or patients; Data analysis and interpretation. XC, ZWZ and BZ—Collection and assembly of data. All authors—Manuscript writing; Final approval of manuscript.

ETHICS APPROVAL AND CONSENT TO PARTICIPATE

This study was approved by Institutional Research Ethics Committee of Fudan University Shanghai Cancer Center (No. 050432-4-1911D) and conducted under the guidance of the Declaration of Helsinki.

ACKNOWLEDGMENT

Not applicable.

FUNDING

This research received no external funding.

CONFLICT OF INTEREST

The authors declare no conflict of interest.

SUPPLEMENTARY MATERIAL

Supplementary material associated with this article can be found, in the online version, at https://oss.ejgo.net/files/article/1780482470537248768/attachment/Supplementary%20material.xlsx.

REFERENCES

[1] Siegel RL, Miller KD, Jemal A. Cancer statistics, 2020. CA: A Cancer Journal for Clinicians. 2020; 70: 7–30.

[2] Lheureux S, Braunstein M, Oza AM. Epithelial ovarian cancer: evolution of management in the era of precision medicine. CA: A Cancer Journal for Clinicians. 2019; 69: 280–304.

[3] Millstein J, Budden T, Goode EL, Anglesio MS, Talhouk A, Intermaggio MP, *et al*. Prognostic gene expression signature for high-grade serous ovarian cancer. Annals of Oncology. 2020; 31: 1240–1250.

[4] Zhao X, He M. Comprehensive pathway-related genes signature for prognosis and recurrence of ovarian cancer. PeerJ. 2020; 8: e10437.

[5] Chen GM, Kannan L, Geistlinger L, Kofia V, Safikhani Z, Gendoo DMA, *et al*. Consensus on molecular subtypes of high-grade serous ovarian carcinoma. Clinical Cancer Research. 2018; 24: 5037–5047.

[6] Teng F, Wei H, Dong X. An immune related signature inhibits the occurrence and development of serous ovarian cancer by affecting the abundance of dendritic cells. Discover Oncology. 2023; 14: 101.

[7] Liu J, Zhang X, Wang H, Zuo X, Hong L. Comprehensive analysis of purine-metabolism-related gene signature for predicting ovarian cancer prognosis, immune landscape, and potential treatment options. Journal of Personalized Medicine. 2023; 13: 776.

[8] Jin Y, Qiu Y, Li Y, Jiang Z, Hu S, Dai H. A novel epithelial-mesenchymal transition-related lncRNA signature predicts prognosis and immune status in endometrioid endometrial cancer. Medicine. 2023; 102: e34126.

[9] Duan Y, Xu X. A signature based on anoikis-related genes for the evaluation of prognosis, immunoinfiltration, mutation, and therapeutic response in ovarian cancer. Frontiers in Endocrinology. 2023; 14: 1193622.

[10] Dong L, Qian Y, Li S, Pan H. Development of a machine learning-based signature utilizing inflammatory response genes for predicting prognosis and immune microenvironment in ovarian cancer. Open Medicine. 2023; 18: 20230734.

[11] Pavlova N, Thompson C. The emerging hallmarks of cancer metabolism. Cell Metabolism. 2016; 23: 27–47.

[12] Xia L, Oyang L, Lin J, Tan S, Han Y, Wu N, *et al*. The cancer metabolic reprogramming and immune response. Molecular Cancer. 2021; 20: 28.

[13] Vaupel P, Schmidberger H, Mayer A. The Warburg effect: essential part of metabolic reprogramming and central contributor to cancer progression. International Journal of Radiation Biology. 2019; 95: 912–919.

[14] Sun L, Zhang H, Gao P. Metabolic reprogramming and epigenetic modifications on the path to cancer. Protein & Cell. 2022; 13: 877–919.

[15] Schiliro C, Firestein BL. Mechanisms of metabolic reprogramming in cancer cells supporting enhanced growth and proliferation. Cells. 2021; 10: 1056.

[16] Ge T, Gu X, Jia R, Ge S, Chai P, Zhuang A, *et al*. Crosstalk between metabolic reprogramming and epigenetics in cancer: updates on mechanisms and therapeutic opportunities. Cancer Communications. 2022; 42: 1049–1082.

[17] Feng Y, Tang Y, Mao Y, Liu Y, Yao D, Yang L, *et al*. PAX2 promotes epithelial ovarian cancer progression involving fatty acid metabolic reprogramming. International Journal of Oncology. 2020; 56: 697–708.

[18] Chen M, Sheng X, Qin Y, Zhu S, Wu Q, Jia L, *et al*. TBC1D8 amplification drives tumorigenesis through metabolism reprogramming in ovarian cancer. Theranostics. 2019; 9: 676–690.

[19] Piga I, Verza M, Montenegro F, Nardo G, Zulato E, Zanin T, *et al*. *In situ* metabolic profiling of ovarian cancer tumor xenografts: a digital pathology approach. Frontiers in Oncology. 2020; 10: 1277.

[20] Zhang Y, Wang Y, Zhao G, Orsulic S, Matei D. Metabolic dependencies and targets in ovarian cancer. Pharmacology & Therapeutics. 2023; 245: 108413.

[21] Zhang D, Li Y, Yang S, Wang M, Yao J, Zheng Y, *et al*. Identification of a glycolysis-related gene signature for survival prediction of ovarian cancer patients. Cancer Medicine. 2021; 10: 8222–8237.

[22] Li H, Qi Z, Niu Y, Yang Y, Li M, Pang Y, *et al*. FBP1 regulates proliferation, metastasis, and chemoresistance by participating in C-MYC/STAT3 signaling axis in ovarian cancer. Oncogene. 2021; 40: 5938–5949.

[23] Jin Y, Bian S, Wang H, Mo J, Fei H, Li L, *et al*. CRMP2 derived from cancer associated fibroblasts facilitates progression of ovarian cancer *via* HIF-1α-glycolysis signaling pathway. Cell Death & Disease. 2022; 13: 675.

[24] Bi J, Bi F, Pan X, Yang Q. Establishment of a novel glycolysis-related prognostic gene signature for ovarian cancer and its relationships with immune infiltration of the tumor microenvironment. Journal of Translational Medicine. 2021; 19: 382.

[25] Nantasupha C, Thonusin C, Charoenkwan K, Chattipakorn S, Chattipakorn N. Metabolic reprogramming in epithelial ovarian cancer. American Journal of Translational Research. 2021; 13: 9950–9973.

[26] Yue H, Lu X. Metabolic reprogramming of the ovarian cancer microenvironment in the development of antiangiogenic resistance. Acta Biochimica et Biophysica Sinica. 2023; 55: 938–947.

[27] Irizarry RA. Exploration, normalization, and summaries of high density oligonucleotide array probe level data. Biostatistics. 2003; 4: 249–264.

[28] Tibshirani R. The lasso method for variable selection in the Cox model. Statistics in Medicine. 1997; 16: 385–395.

[29] Van Nyen T, Planque M, van Wagensveld L, Duarte JAG, Zaal EA, Talebi A, *et al*. Serine metabolism remodeling after platinum-based chemotherapy identifies vulnerabilities in a subgroup of resistant ovarian cancers. Nature Communications. 2022; 13: 4578.

[30] Tian X, Han Y, Yu L, Luo B, Hu Z, Li X, *et al*. Decreased expression of ALDH5a1 predicts prognosis in patients with ovarian cancer. Cancer Biology & Therapy. 2017; 18: 245–251.

[31] Mogami T, Yokota N, Asai-Sato M, Yamada R, Koizume S, Sakuma Y, *et al*. Annexin A4 is involved in proliferation, chemo-resistance and migration and invasion in ovarian clear cell adenocarcinoma cells. PLOS ONE. 2013; 8: e80359.

[32] Lv XF, Hong HQ, Liu L, Cui SH, Ren CC, Li HY, *et al*. RNAi-mediated downregulation of asparaginase-like protein 1 inhibits growth and promotes apoptosis of human cervical cancer line SiHa. Molecular Medicine Reports. 2018; 18: 931–937.

[33] Rankin EB, Fuh KC, Taylor TE, Krieg AJ, Musser M, Yuan J, *et al*. AXL is an essential factor and therapeutic target for metastatic ovarian cancer. Cancer Research. 2010; 70: 7570–7579.

[34] Fukumoto T, Zhu H, Nacarelli T, Karakashev S, Fatkhutdinov N, Wu S, *et al*. N^6-Methylation of adenosine of *FZD10* mRNA contributes to PARP inhibitor resistance. Cancer Research. 2019; 79: 2812–2820.

[35] Lin T, Chen S, Huang M, Huang J, Hsu C, Juan H, *et al*. GALNT6 expression enhances aggressive phenotypes of ovarian cancer cells by regulating EGFR activity. Oncotarget. 2017; 8: 42588–42601.

[36] Zhang J, Yang L, Xiang X, Li Z, Qu K, Li K. A panel of three oxidative

stress-related genes predicts overall survival in ovarian cancer patients received platinum-based chemotherapy. Aging. 2018; 10: 1366–1379.

[37] Zhao H, Sun Q, Li L, Zhou J, Zhang C, Hu T, *et al*. High expression levels of AGGF1 and MFAP4 predict primary platinum-based chemoresistance and are associated with adverse prognosis in patients with serous ovarian cancer. Journal of Cancer. 2019; 10: 397–407.

[38] Huang Y, Dai Z, Barbacioru C, Sadée W. Cystine-glutamate transporter SLC7A11 in cancer chemosensitivity and chemoresistance. Cancer Research. 2005; 65: 7446–7454.

[39] Park K, Kim H, Lee J, Choi Y, Park S, Yang S, *et al*. Transglutaminase 2 as a cisplatin resistance marker in non-small cell lung cancer. Journal of Cancer Research and Clinical Oncology. 2010; 136: 493–502.

How to cite this article: Yaodong Zhang, Xuenan Zhao, Huilan Qiu, Xia Chen, Zhongwei Zhang, Biao Zhu, *et al*. Metabolism related gene signature predicts prognosis and indicates tumor immune infiltration in ovarian cancer. European Journal of Gynaecological Oncology. 2024. doi: 10.22514/ejgo.2024.040.